ELSEVIER

Journal of Alloys and Compounds 374 (2004) 190–193

Journal of ALLOYS AND COMPOUNDS

www.elsevier.com/locate/jallcom

Influence of the precursor purity and the precipitating agent on impedance spectroscopy of CeO_2:Y_2O_3 ceramics

S.K. Tadokoro*, E.N.S. Muccillo

Centro Multidisciplinar para o Desenvolvimento de Materiais Cerâmicos, Instituto de Pesquisas Energéticas e Nucleares—CCTM, C.P. 11049-Pinheiros, São Paulo 05422-970, SP, Brazil

Abstract

In this work, yttria-doped ceria solid solutions were prepared to produce dense ceramic specimens with high chemical and microstructural homogeneities, and with high ionic conductivity. Cerium nitrate with different degrees of purity and yttrium oxide were used as starting materials. The co-precipitation technique was performed using either ammonium hydroxide or oxalix acid as precipitating agent. The main results show that the preparation of nanosized powders of yttria-doped ceria does not depend on the precipitating agent used during synthesis. The average grain sizes are found to be different in sintered specimens prepared from powders following the two routes, thereby affecting the electrical resistivity measured by impedance spectroscopy. The intergranular conductivity is also dependent on the purity of the precursor material.

Keywords: Precipitation; X-ray diffraction; Ionic conduction

1. Introduction

Pure and doped ceria have attracted much attention because of their many practical uses, such as automobile exhaust catalysts, mechanical polishing media, and additives in ceramic processing [1–3]. More recently, high-technology applications have emerged [4]. These applications of doped ceria ceramics take advantage of the high oxygen-ion conduction in these materials.

In an oxygen-ion conducting material the total electrolyte conductivity may be divided in two components: intragranular and intergranular. The intragranular component is related to the capacitance and resistance of the bulk material, whereas the intergranular component is related to the conduction through interfaces between grains. As a common feature in oxygen-ion conducting materials, the intergranular conductivity decreases with increasing impurity content and grain boundary surface area [5]. There is no definitive model to quantitatively describe the role of impurity phases and how they influence ionic conduction across grain boundaries. However, based on experimental evidence in the literature, it is reasonable to assume that they may have a deleterious effect on the total ionic conductivity of a solid electrolyte [5,6].

Earlier studies on this subject in ceria-based solid solutions have shown that an amorphous glassy phase at the grain boundaries could account for the low intergranular conductivity of these ceramics [7,8]. The effect of dopant segregation at the grain boundaries was also claimed as another possible reason for this phenomenon [9]. However, electron microscopy observations have shown that there were no secondary phases present at the grain boundaries, although the intergranular conductivity was lower than that of the bulk material by a factor of 1000, in the 250–500 °C temperature range [10]. Using a combination of Z-contrast imaging and electron energy-loss spectroscopy, it was recently shown that in gadolinium-doped ceria there was an increase in the number of charge carriers (oxygen vacancies) in the grain boundary core that was partially compensated by dopant segregation [11]. In contrast, scanning transmission electron microscopy results in yttria-doped ceria point to a depletion of oxygen-ion vacancies in the grain boundary area [12].

In these previous studies the effects of grain growth and the corresponding evolution of the grain boundary surface area on the intergranular component of the ionic conductivity were not taken into account. In this study, these effects were studied on yttria-doped ceria by impedance spectroscopy aiming to obtain a better knowledge of the low-conductivity intergranular component in this ceramic material.

* Corresponding author. Fax: +55-11-38169370.
E-mail address: sktadok@ipen.br (S.K. Tadokoro).

0925-8388/$ – see front matter © 2003 Elsevier B.V. All rights reserved.
doi:10.1016/j.jallcom.2003.11.090

2. Experimental

$Ce(NO)_3{\cdot}6H_2O$ (99.9%, Strem Chemicals, 99.99 and 99.999%, Aldrich Chemicals) and Y_2O_3 (99.99%, Sigma Chemicals) were used as precursor materials. A stock solution of yttrium nitrate was prepared by dissolving the yttrium oxide precursor in a nitric acid solution under heating and stirring. The concentration of this solution was verified by gravimetry.

Solid solutions of ceria–8 mol%-yttria were prepared by co-precipitation using ammonium hydroxide or oxalic acid, both of analytical grade, as precipitating agent. The nitrate precursor solutions were mixed in the required proportion. The mixed nitrate solution (1.0 mol l^{-1}) was dipped onto the precipitating agent solution. The pH of precipitation was fixed at 6.5 and 10 for the oxalate and hydroxide co-precipitation, respectively. After digestion for 15 min, the coprecipitate was washed with deionized water and filtered under vacuum for three times. The dehydration was carried out by washing with ethyl alcohol and isopropyl alcohol, followed by distillation with *n*-butyl alcohol. Further details on the co-precipitation process can be found elsewhere [13]. The co-precipitate was calcined at 400 °C. Cylindrical specimens were prepared by pressing at 196 MPa and sintering at 1500 °C for 4 h.

Characterization of the powdered material was carried out by nitrogen adsorption (ASAP 2010, Micromeritics) to determine specific surface area (S) values by the BET method. X-ray diffraction (XRD) patterns were recorded using a diffractometer (D8 Advance, Bruker-AXS) equipped with a Ni-filtered Cu K_α radiation source. The range of scans were 20–80° 2θ for crystalline phase identification and 25–31° 2θ for crystallite size, t_{XRD}, measurements. Crystallite sizes were estimated from the (1 1 1) reflection using the Scherrer equation [14]. Apparent density (d_h) values in sintered specimens were measured using the Archimedes principle. Polished and thermally etched surfaces of sintered ceramics were observed with the help of scanning electron microscopy (XL30, Philips) for grain size (G) measurements. Silver paste was used as electrode material for electrical measurements. Electrical resistance (R) measurements were carried out on sintered specimens using an LF impedance analyzer (4192A, Hewlett Packard) in the 5 Hz to 13 MHz frequency range. Electrical conductivity (σ) values for sintered specimens were calculated from the measured resistance by $\sigma = k/R$, where k is the ratio between the specimen thickness and the electrode area.

3. Results and discussion

Values of specific surface area for calcined powders are shown in Table 1. Relatively high values were obtained independent on the precipitating agent used. However, the co-precipitation of yttrium and cerium by the hydroxide route resulted in powders with the highest value of specific surface area.

Table 1
Values of specific surface area, crystallite size, apparent density and grain size for materials prepared by hydroxide and oxalate co-precipitation

Route	S ($m^2\,g^{-1}$)	t_{XRD} (nm)	Density ($g\,cm^{-3}$)	G (μm)
Hydroxide	180.9	5.80	6.6	6.5
Oxalate	110.0	5.84	6.5	4.3

XRD patterns are shown in Fig. 1. The dried hydroxide coprecipitate was crystalline in nature, whereas the oxalate coprecipitate consisted of an amorphous material. After thermal treatments no qualitative differences were observed in the XRD patterns of specimens, and only those of oxalate precursor are shown in this figure. X-ray diffraction patterns after calcination at 400 °C for 1 h reveal line broadening showing that crystallite sizes remain small. Values of crystallite size are shown in Table 1. It is worth noting the similarity in these figures, besides the difference in specific surface area values. This effect may be due to different particle shapes. Similar values for the crystallite size are reported in the literature [15], which is an indication that nanosized powders may be obtained independent on specific parameters used during synthesis. After sintering at 1500 °C for 4 h, XRD patterns exhibit sharp reflections due to an increase of the crystallite size.

The apparent density of sintered specimens (Table 1) is essentially independent on the precipitating agent used. However, the average grain size of specimens prepared by the oxalate precipitation is 50% lower than that of specimens prepared by the hydroxide route.

Representative impedance diagrams of specimens prepared by the oxalate co-precipitation, but with different purity of the precursor material are shown in Fig. 2. Numbers in these diagrams are the decimal logarithm of the frequency,

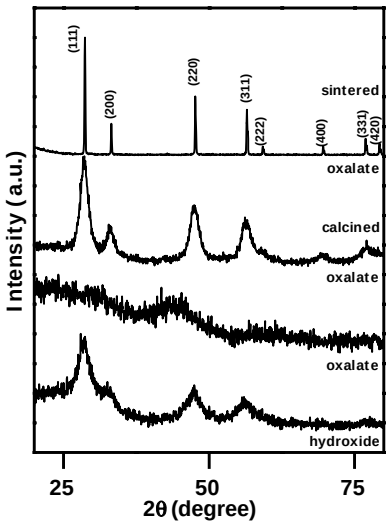

Fig. 1. X-ray diffraction patterns, from bottom to top, of dried (hydroxide and oxalate), calcined (oxalate), and sintered (oxalate) specimens.

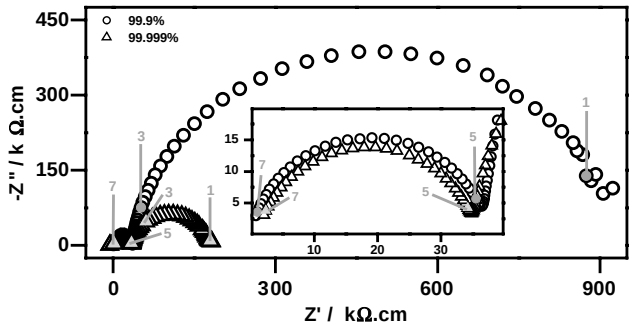

Fig. 2. Impedance diagrams of specimens prepared by the oxalate co-precipitation with different purity of the cerium precursor material. The inset shows the high frequency (intragranular) region.

and the temperature of measurement was 260 °C. It should be noted in these diagrams, that the high-frequency semicircles do not differ significantly meaning equal values of intragranular resistivity. The low-frequency semicircles, on the contrary, have different diameters, giving rise to different values of intergranular resistivity.

Fig. 3 shows Arrhenius plots of the intragranular and intergranular components of the electrolyte conductivity for all specimens studied. The intragranular conductivity does not depend on the precursor purity or the precipitating agent. This result is a consequence of high chemical and microstructural homogeneities inside grains in these polycrystalline ceramics. In contrast, the intergranular component of the conductivity depends on the precipitating

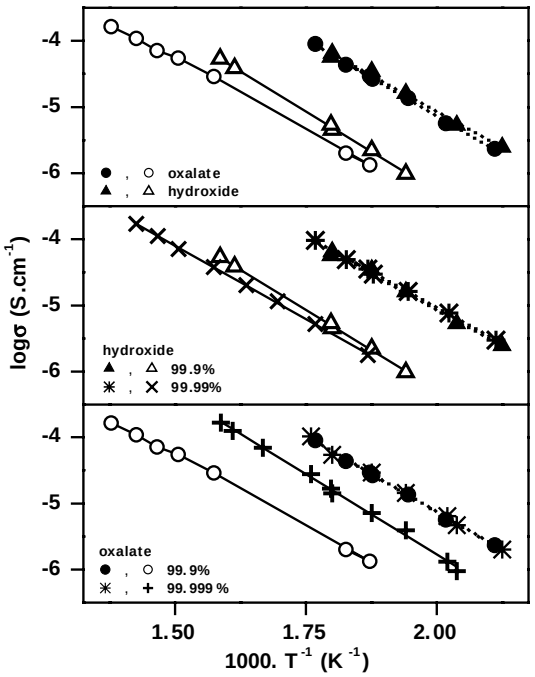

Fig. 3. Arrhenius plots of intragranular (filled symbols, ✳) and intergranular (×, + and open symbols) components of the electrical conductivity for specimens prepared by different routes and different purity of the cerium precursor.

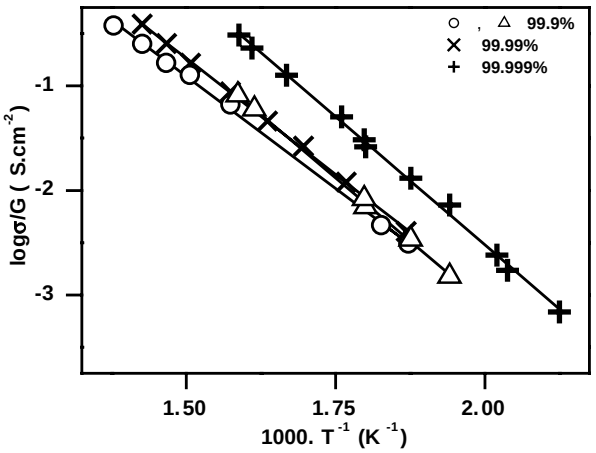

Fig. 4. Arrhenius plots of the intergranular conductivity normalized for the grain size.

agent and on the purity of the precursor material. It can be observed that for cerium precursors with impurity contents 100 and 1000 ppm, the difference between the corresponding intergranular conductivities is low. However, for the precursor with higher degree of purity, this difference is not negligible. For a fixed temperature, the ratio between intergranular and intragranular conductivities varies from ∼15 to ∼25, except for the cerium precursor with 99.999%. In this case, this ratio is approximately 4.

Fig. 4 shows Arrhenius plots of the intergranular conductivity after correction for the grain size effect. It can be seen that the intergranular conductivity is, within experimental errors, approximately the same for all specimens, except for that prepared with the cerium precursor of the highest degree of purity.

These results demonstrate that a high purity cerium precursor is required to improve the total electrical conductivity of yttria-doped ceria ceramics.

4. Conclusions

Nanosized powders of yttria-doped ceria with high chemical homogeneity were prepared by the co-precipitation technique. High values of specific surface area and low values of average crystallite size were obtained, indicating that high sinteractive powders were prepared. High densification of pressed specimens was obtained by sintering at 1500 °C for 4 h. The conductivity of the bulk material is insensitive to all studied parameters. The intergranular component of the electrical conductivity proved to be dependent on the grain size of sintered specimens, and on the purity of the precursor material.

Acknowledgements

Authors thank FAPESP (95/05172-4, 96/09604-9, 99/04929-5), CNPq (300934/94-7), PRONEX and CNEN for

financial support. S.K. Tadokoro acknowledges FAPESP for the scholarship (00/08908-1).

References

[1] B.R. Powel, R.L. Bloink, C.C. Erkel, J. Am. Ceram. Soc. 71 (1988) C104.
[2] N.B. Kirk, J.V. Wood, Br. Ceram. Trans. 93 (1994) 25.
[3] A. Trovarelli, C. de Leitenburg, M. Boaro, G. Dolcetti, Catal. Today 50 (1999) 353.
[4] K. Eguchi, T. Setoguchi, T. Inoue, H. Arai, Sol. State Ion. 52 (1992) 165.
[5] S.P.S. Badwal, Sol. State Ion. 76 (1995) 67.
[6] M. Mogensen, N.M. Sammes, G.A. Tompsett, Sol. State Ion. 129 (2000) 63.
[7] J.A. Kilner, B.C.H. Steele, in: O.T. Sorensen (Ed.), Non-Stoichiometric Oxides, Academic Press, New York, 1981.
[8] R. Gerhardt, A.S. Nowick, M.E. Mochel, I. Dumler, J. Am. Ceram. Soc. 69 (1986) 647.
[9] K. El Adham, A. Hammou, Sol. State Ion. 9 (1983) 905.
[10] G.M. Christie, F.P.F. van Berkel, Sol. State Ion. 83 (1996) 17.
[11] Y. Lei, Y. Ito, N.D. Browning, T.J. Mazanec, J. Am. Ceram. Soc. 85 (2002) 2359.
[12] X. Guo, W. Sigle, J. Maier, J. Am. Ceram. Soc. 86 (2003) 77.
[13] S.K. Tadokoro, E.N.S. Muccillo, J. Alloy Comp. 344 (2002) 186.
[14] B.E. Warren, in: X-ray Diffraction, Dover, New York, 1990, p. 258.
[15] S. Zha, Q. Fu, Y. Lang, C. Xia, G. Meng, Mater. Lett. 47 (2001) 351.